Reproductive Biology and Endocrinology

RESEARCH

Open Access

ViLR: a novel virtual long read method for breakpoint identification and direct SNP haplotyping in *de novo* PGT-SR carriers without a proband

Jiangyang Xue[1,2,3†], Min Xie[1,2,3†], Jie Cai[4], Kai Kang[5], Mengnan Gu[5], Mai Li[4], Haiyue Shi[4], Xin Zhang[5], Lingyin Kong[5], Bo Liang[6], Liming Zhou[4], Changshui Chen[2*] and Haibo Li[1,2,3*]

Abstract

Background Despite the gradual application of third-generation long read sequencing (LRS) or reference embryo establishment to preimplantation genetic testing for structural rearrangement (PGT-SR) without familial involvement, there are still limitations to their extensive clinical application yet. This study developed a novel virtual NGS-based long read method (ViLR) and preliminarily evaluated its clinical feasibility of breakpoint characterization and direct SNP haplotyping for *de novo* chromosomal structural rearrangements (CSR).

Methods A total of 10 families with *de novo* CSR risk were enrolled in this study for ViLR analysis. In contrast to LRS, ViLR is a virtual long read solution that used the same barcoded labeling and assembly of different long gDNAs differently barcoded. Notably, ViLR could generate an average fragment length of over 30 Kb, with an N50 block size of up to 16 Mb in a single assay, allowing to achieve accurate breakpoint mapping and direct carrier's haplotyping. An approximately 2 Mbp region flanking upstream and downstream of each breakpoint was selected for informative SNP collection. Embryo haplotype determination was based on the established carriers' haplotypes after whole genome amplification and sequencing. To confirm PGT-SR results, we performed prenatal genetic diagnosis.

Results This study achieved an average mapping rate of 99.5%, > 90% coverage depth (> 10X), an average number of effective barcode (> 5 kb length) counts of 11,000,000 and an average fragment length of 40 kb, which generated sufficient informative SNPs for breakpoint characterization and haplotype phasing. ViLR analysis of 10 *de novo* PGT-SR carriers precisely identified breakpoints and haplotypes. Seven families obtained 18 euploid embryos, in which 10 were euploid/normal embryos, 7 were euploid/balanced carrier embryos, and the remaining one unknown was due to homologous recombination of the breakpoint region. Prenatal genetic diagnosis was performed for four women,

†Jiangyang Xue and Min Xie contributed equally to this work.

*Correspondence:
Changshui Chen
chencs@139.com
Haibo Li
lihaibo-775@163.com

Full list of author information is available at the end of the article

and the outcomes coincided with the results from embryo PGT-SR. At the time of writing this paper, four healthy babies had been delivered uneventfully.

Conclusion Here, we demonstrated the clinical potential of ViLR as a novel solution for breakpoint identification and direct SNP haplotyping in *de novo* PGT-SR families without proband involvement.

Clinical trial number Not applicable.

Keywords Virtual NGS-based long read method (ViLR), Breakpoint identification, Direct SNP haplotyping, *De novo*, Preimplantation genetic testing for structural rearrangement (PGT-SR)

Background

Balanced translocation (BT) and inversion, both considered chromosomal structural rearrangements (CSR), are common genetic causes for assisted reproductive technology (ART) [1, 2]. A recent retrospective study indicated that the overall prevalence of chromosome aberrations was 2.04% in 17,054 Chinese infertile patients, of which 0.97% were BT carriers and 0.09% had inversions [3]. Carriers with BT or inversion are usually phenotypically normal, but prone to produce imbalanced gametes, resulting in recurrent spontaneous abortions, implantation failure, infertility, or fetal defects [4, 5]. Preimplantation genetic testing for structural rearrangements (PGT-SR) allows selecting disease-free embryos to transfer in CSR carriers [6]. Traditionally, embryo diagnosis could be achieved via next-generation sequencing (NGS) or single nucleotide polymorphism (SNP) microarray-based genome-wide haplotyping relying on an affected proband or other inherited relatives in the family [7–9], which might be a great challenge for *de novo* PGT-SR pedigrees without available family samples.

Although the percentage of *de novo* CSR carriers in the general population or infertile couples is so far unreported, the actual carrier burden may be underestimated as individuals with incomplete families are usually managed as *de novo* genotypes in practical clinical PGT-SR. However, the informative SNPs for direct carrier haplotyping could be insufficient when using traditional linked short-read NGS technology. Thus, optimized NGS-based strategies for direct independent embryo testing, such as whole genome sequencing (WGS) based on parent-embryo haplotypes [10], low depth WGS-based comprehensive PGT [11], or GENType [9], have been recently implemented to establish a reference haplotype. However, these techniques are limited by the high number of embryos needed to achieve an accurate haplotype. According to Ou's study, having an affected embryo that allows haplotype phasing was a matter of probability. Even with 8 embryos, there was still a 10% chance that no reference embryos were available [12]. An impaired ovarian reserve or diminished sperm quality may decrease the available blastocysts, or the reference embryo could not be accessible due to failed direct genotyping. In addition, PCR errors or allelic dropout (ADO) are unavoidable during whole genome amplification (WGA) of direct embryo detection.

Currently, third-generation long read sequencing (LRS) technologies, mainly from Pacific Biosciences (PacBio) and Oxford Nanopore Technologies (ONT), have the unique advantage of ≥10 kb long readings to obtain a direct accurate haplotype in CSR families. For instance, the PacBio platform could provide a useful set of SNPs in PGT-SR and preimplantation genetic testing for monogenic disease (PGT-M) test designs [13]. Similarly, previous studies demonstrated the utility of ONT's platform in haplotyping inversion and BT carriers [14, 15]. Moreover, Tsuiko proposed that LRS application could help with preclinical haplotype imputation of couples with *de novo* variants [16]. Nevertheless, the high sequencing cost limits its extensive clinical applicability of LRS. For instance, a single human genome sequencing run (30× depth) using LRS costs $1,000–2,000, generally 5–10 times higher than with linked short-read NGS [17]. Therefore, an efficient and cost-effective NGS-based detection platform is needed for direct haplotyping in single *de novo* carriers without a proband.

We developed a novel virtual NGS-based long-link read method (ViLR) for an average fragment length of over 30 Kb per molecule, based on the same barcoded labeling. Assembly and alignment of different long gDNAs with different barcodes after sequencing produced sufficient informative SNPs for mapping to the reference genome. We collected a total of 10 *de novo* PGT-SR pedigrees (8 BTs and 2 inversions) in this prospective design. Each carrier underwent ViLR analysis for breakpoint characterization and direct SNP haplotyping. Linkage analysis and embryo genotype identification were based on the established carriers' haplotypes. Overall, our study demonstrated the clinical feasibility and applied potential of ViLR for *de novo* PGT-SR pedigrees without familial involvement.

Methods

Sample information

A total of 10 families with CSR risk were collected and subjected to intracytoplasmic sperm injection (ICSI) and PGT-SR at the Affiliated Women and Children's Hospital of Ningbo University. Written informed consent

was obtained from all participants, and this study was approved by the IRB of the Affiliated Women and Children's Hospital of Ningbo University (No. EC2020-048). The study adhered to the provisions of the Declaration of Helsinki as revised in 2013.

In these families, one of the couples were BT or inversion carriers, whose chromosomal rearrangements were primarily determined by G-banded karyotyping (KT) and diagnosed as *de novo* carriers after parental KT validation and paternity testing. The description of karyotypes referred to an International System for Human Cytogenomic Nomenclature 2024 [18]. No probands (an affected offspring with genetic abnormalities already presented in the family) were found in 10 families. Chromosomal breakpoints and genetic haplotypings were further analyzed with ViLR, instead of traditional familial SNP haplotyping. The carriers' genetic information, including KT description, breakpoints, implantation decision-making and pregnancy outcome, are displayed in Table 1. Nine families obtained their embryos through ICSI, and blastocysts were biopsied to screen for the optimal embryo for implantation. The embryos' genetic information, such as haplotype, presence of chromosomal aberrations, which embryo to select, as well as the cytogenetic result of amniotic fluid, are shown in Table 2.

Long gDNA treatment and sequencing

High molecular weight (HMW) gDNA samples were extracted from peripheral blood by Nanobind HMW DNA Extraction-Mammalian Whole Blood kit (Circulomics, USA). The concentration was measured by the Qubit™ dsDNA High Sensitivity (HS) Assay Kit (Thermo Fisher Scientific, USA); the qualified gDNA concentration was usually ≥ 10 ng/μL. A total of 10 ng gDNA was used for library construction.

Briefly, a gDNA library was constructed by adding sample labels, barcoded beads, adapters and through PCR amplification. Initially, long gDNAs were randomly inserted by sample label (through a transposome carried with the transposon). Each barcoded bead was premarked with around 400,000 identical DNA tags. The complementary oligo sequences on both transposons and barcoded beads could facilitate bilateral connection through a ligase. Eventually, a long gDNA was bound with tag-marked barcoded beads; thus, reads from one long gDNA were marked with the same tags and different long gDNAs with different tags. Thereafter, spare oligos were digested, the transposome deactivated, and adapters added. Short DNA fragments with the same tags were derived from a long DNA molecule. Finally, the libraries were built by PCR amplification (Fig. 1).

The concentration and fragment size of libraries were quantified using the Qubit™ dsDNA HS Assay Kit and 2100 High Sensitivity DNA Kit (Agilent, United States). The concentration of qualified libraries should be ≥ 2.6 ng/μL, and the fragment size distributed across 200–2000 bp. A MGI-2000 sequencer (MGI Tech Co., Ltd., ShenZhen, China) was used for genome sequencing. The data generated from all samples is shown in Supplementary Tables 1–2.

Table 1 Genetic information of carriers examined with ViLR

Pedigree No.	Carrier gender	Genetic description of karyotyping	Breakpoints by ViLR analysis (hg 19)	Disrupted gene breakpoints (intragenic/intergenic)	Phase of clinical PGT-SR cycle
PSJ22007	Male	46,XY, t(2;15)(p21;q26.1)	chr2: 36,702,101; chr15: 100,682,799	CRIM1: intron5; ADAMTS17: intron10	Prenatal diagnosis finished and a healthy baby delivered
PSJ22019	Male	46,XY, t(1;7)(q42;q11.2)	chr1: 235,334,249; chr7: 77,004,459	ARID4B: intron23; GSAP: intron10	No available embryos
PSJ22015	Male	46,XY, t(3;22)(q24;q12)	chr3: 132,423,676; chr22: 20,655,812	NPHP3: intron8; FAM230J: intron1	No available embryos
PSJ23002	Male	46,XY, t(6;13)(p21.1;p12)	chr6: 42,996,416; chr13: undetectable	RRP36: intron6; undetectable	Failed ET at the first cycle
PSJ23008	Female	46,XX, t(8;17)(p23.2;q25)	chr8: 3,146,675; chr17: 74,040,722	CSMD1: intron25; SRP68: intron11	Prenatal diagnosis finished and a healthy baby delivered
PSJ23011	Female	46,XX, inv(7)(p14q21)	chr7: 33,669,203; chr7: 86,843,221	BBS9: intron22; TMEM243: intron2	Prenatal diagnosis finished and a healthy baby delivered
PSJ23012	Male	46,XY, t(1;18)(q24;q21.2)	chr1: 176,251,882; chr18: 58,488,969	COP1-PAPPA2 (intergenic); MC4R-CDH29 (intergenic)	Prenatal diagnosis finished and a healthy baby delivered
PSJ23019	Female	46,XX, t(1;11)(p22;p13)	chr1: 90,088,859; chr11: 33,317,308	LRRC8B-LRRC8C-DT (intergenic); HIPK3: intron2	Abortion at gestational age of 7 weeks with unknown reason
PSJ23021	Male	46,XY, t(7;22)(p15;q11.2)	chr7: 23,030,769; chr22: 18,976,664	FAM126A: intron1; DGCR5: intron2	Had not been involved in ovarian stimulation cycle
PSJ24002	Female	46,XX, inv(20)(p13q11.2)	chr20: 6,582,577; chr20: 31,663,698	CASC20-LINC01713 (intergenic); BPIFB3-BPIFB4 (intergenic)	Successful pregnancy but inaccessible prenatal diagnosis

Table 2 Genetic information of biopsied blastocysts

Pedigree No.	Embryo No.	Embryo morphology	Haplotype result	Embryonic CNV result	Embryo selection	Cytogenetic result of amniotic fluid
PSJ22007	E1	4BB	Carrier	del(mosaic)(20)(p13p11.23)(67%); del(mosaic)(X)(q21.2q28)(34%)		
	E2	4BC	Normal	+4		
	E3	4BC	Normal	46,XN	√	Normal
PSJ22019	E1	4BB	Unbalanced	dup(1)(q42.3q44); del(7)(q11.23q36.3); del(mosaic)(11)(q13.4q25)(47%)		
	E2	4BB	Carrier	-(mosaic)(20)(44%)		
	E3	4BC	Unbalanced	dup(1)(q42.3q44); del(7)(q11.23q36.3)		
PSJ22015	E1	4BB	Normal	del(mosaic)(9)(q21.11q34.3)(32%)		
PSJ23002	E1	4BB	Unbalanced	dup(6)(p25.3p12.3)		
	E2	4BB	Normal	46,XN*	√	No pregnancy
	E3	4BB	Unknown	Failed quality control		
	E4	4BB	Normal	+(mosaic)(4)(34%); +(mosaic)(16)(58%)		
	E5	4BC	Normal	46,XN*		
	E6	4BC	Unbalanced	-X; del(5)(q11.1q35.3); dup(6)(p25.3p12.3)		
PSJ23008	E1	4BB	Normal	-15		
	E2	4BB	Normal	46,XN	√	Normal
	E3	4BB	Unbalanced	dup(8)(p23.3p23.2); del(17)(q25.1q25.3)		
	E4	4BC	Unbalanced	dup(8)(p23.3p23.2); del(17)(q25.1q25.3); del(mosaic)(14)(q11.2q32.32)(30%)		
	E5	5BC	Normal	46,XN		
	E6	4BC	Normal	46,XN		
PSJ23011	E1	4AB	Normal	dup(5)(q31.3q35.3); del(16)(p13.3p11.2)		
	E2	4AB	Normal	+(mosaic)(18)(42%); +(mosaic)(22)(41%); +(mosaic)(X)(36%)		
	E3	4BB	Normal	46,XN	√	Normal
	E4	4BB	Carrier	+11		
	E5	4BB	Normal	46,XN		
	E6	4BB	Carrier	46,XN		
	E7	4BB	Unknown	46,XN		
	E8	4BB	Normal	+(mosaic)(6)(45%); +(mosaic)(19)(51%)		
	E9	4BB	Carrier	46,XN		
	E10	4BC	Normal	del(3)(p26.3p12.3)		
	E11	4BC	Carrier	46,XN		
	E12	4BC	Normal	46,XN		
PSJ23012	E1	4BB	Carrier	-16		
	E2	4BB	Unbalanced	-17; del(1)(q25.2q44); del(18)(p11.32q21.32)		
	E3	4BC	Carrier	46,XN	√	Carrier
	E4	4BC	Normal	-(mosaic)(18)(64%)		
	E5	4BC	Unbalanced	dup(1)(p36.33q25.2); del(18)(p11.32q21.32)		
PSJ23019	E1	4BB	Carrier	46,XN		
	E2	4BB	Normal	46,XN	√	Abortion
PSJ24002	E1	4BB	Carrier	46,XN	√	
	E2	4BB	Carrier	46,XN		
	E3	4BC	Normal	dup(mosaic)(9)(p24.3p21.2)(48%)		

*Aneuploidy of the short arm of chr13 could not be ruled out

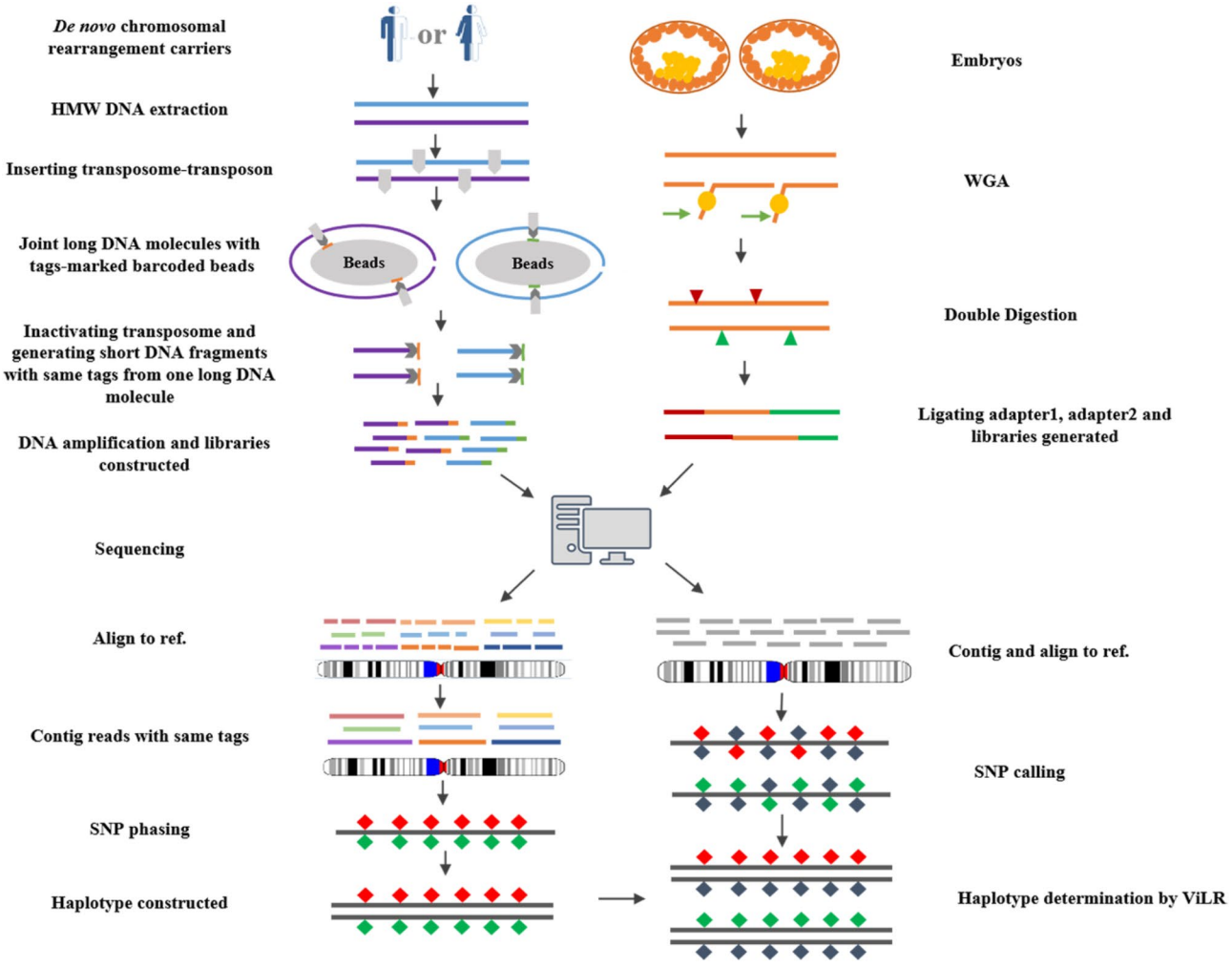

Fig. 1 Overview of ViLR workup strategy. ViLR is a novel virtual NGS-based long-link read method, firstly developed for *de novo* PGT-SR carriers' haplotype phasing without a proband. (1) Specifical sample and barcoded bead labeling. First, HMW gDNAs were extracted from *de novo* chromosomal rearrangement carriers. Long gDNAs were inserted by transposome-transposon, and linked with tags-marked barcoded beads. After inactivating the transposome and adding the adapters, short DNA fragments with the same tags were generated. Finally, libraries were built by PCR amplification. (2) Breakpoint identification and direct SNP haplotyping of carriers. After sequencing, a long read gDNA with the same tags could be assembled; different long read molecules differently tagged were simultaneously generated and aligned for mapping to the reference genome. Sufficient informative SNPs were collected for breakpoint characterization and haplotype phasing. (3) Haplotype determination of embryos. Blastocysts were subjected to biopsy and WGA. After genome library construction, sequencing and SNP calling, embryonic haplotypes could be directly identified based on the established carriers' haplotype phasing

Carriers' chromosomal breakpoints confirmation

Raw sequencing FASTQ files were trimmed by removing DNA molecular tag sequences and the tag information embedded onto read names using a predefined table. We filtered low quality reads with adaptors or bases with quality Q10 ≥ 10%. The BWA software (version 0.7.17-r1188) was used to align the preprocessed files against the reference genome (GRCh37/hg19), resulting in the generation of BAM files containing aligned reads. Post-alignment, PCR deduplication and base quality score recalibration were performed using the GATK software (v4.1.4.0-local), and mutations were analyzed to produce single nucleotide variant vcf files. Smoove software (version 0.2.8) was employed to determine breakpoints and genotype information of structural variants (SVs). The diagram of reads alignment around the breakpoint regions is displayed in Supplementary Tables 3–11.

Carriers' haplotype phasing without a proband

HapCut2 software (v1.3.1) was used for assembling and haplotyping target SV chromosomes. Reads inferred SV breakpoints were used to identify SV-carrying haplotypes by phased tags of read names from Hapcut2 results. To distinguish paternal and maternal alleles, informative SNPs were selected based on parental genotypes,

focusing on heterozygous SNPs in the carrier parent and homozygous SNPs in the other parent.

ICSI and trophectoderm biopsy

All these families received ART due to SV risk. To integrate mature oocytes, fertilization was completed by ICSI. Two pronuclei were considered normal after 16–18 h, and embryos were cultured until ≥4 cells on D3. Blastocysts with morphology ≥ 3BC according to the Gardner and Schoolcraft grading system were subjected to trophectoderm biopsy at D5 or D6. A total of 3–5 cells were obtained from each blastocyst and added to 2 μL of phosphate-buffered saline. The preparations were frozen at -20°C and immediately vitrified.

Sequencing and genotypes identification for embryos

Embryonic samples were processed by a REPLI-g Single Cell Kit (150345, QIAGEN, Germany) for multiple displacement amplification (MDA)-based WGA according to the manufacturer's instructions. An integrated haplotyping-based approach involving DNA library construction, sequencing and data analysis was applied for embryo PGT [19]. The output of each sample was ≥ 8 GB and had a Q30 > 80%.

The embryonic sequencing data were aligned to human reference genome (National Center for Biotechnology Information hg19 version) via BWA (Burrows-Wheeler-Alignment Tool, http://bio-bwa.sourceforge.net/). GATK (Genome Analysis Tool Kit, http://www.broadinstitute.org/gatk/) was used to identify SNPs in the genome. Then the SNP sites of the embryo could be used for embryo haplotype analysis. An approximately 1 Mbp region flanking upstream and downstream of each breakpoint was selected for ADO loci and total phasing SNP loci calculating, and the ratio of two values was defined as ADO rate. Based on informative SNPs from carriers' haplotypes, structural rearrangements in the embryos' chromosomes were identified by SNP haplotype analysis. Embryos exhibiting unbalanced chromosomal rearrangements based on copy number variation were excluded from SNP haplotype analysis. Balanced embryos exhibiting phased SNPs consistent with SV-carrier haplotypes were diagnosed as euploid/balanced carrier embryos, while the others were classified as euploid/normal embryos.

Embryo transfer and prenatal diagnosis

Only euploid/normal and euploid/balanced embryos were considered as available embryos for transplantation. Combined with embryo morphology results, one optimal embryo was selected to transferred into the uterus (Table 2). Except for Pedigree PSJ23012 and PSJ24002, other five transplantable families were implanted with euploid/normal embryos. Amniocentesis was performed at week 19 of gestation. KT and chromosomal microarray analysis of amniotic fluid samples were diagnosed to confirm PGT-SR results.

Results

Genetic description of 10 *de novo* CSR carriers

From June 2022 to January 2024, a total of 10 families with *de novo* chromosomal rearrangements requesting PGT-SR were enrolled in this prospective study. The genetic abnormalities of 10 carriers had been previously determined by conventional KT analysis. Only two females carried chromosomal pericentric inversions, while the remaining eight carriers were BTs. Moreover, as no probands or other relatives were available, ViLR analysis was used for breakpoint identification and direct SNP haplotyping of 10 carriers. A total of 19 breakpoints were identified, of which 14 were located within intragenic intron regions, and five were intergenic. Regarding the clinical PGT-SR phase, seven families obtained available embryos for transplantation, four passed prenatal diagnosis, and successfully delivered healthy babies (Table 1).

Breakpoint identification and direct SNP haplotyping with ViLR analysis

An overview of ViLR is shown in Fig. 1. The genome sequencing data in this study achieved an average mapping rate of 99.5%, > 90% coverage depth (> 10X), an average number of effective barcode (> 5 kb length) counts of 11,000,000 and an average fragment length of 40 kb (Supplementary Table 1), which generated sufficient informative SNPs for subsequent breakpoint characterization and haplotype phasing.

As shown in the PSJ22007 carrier, breakpoint locations and chromosome translocations could be precisely detected by ligation of various different barcodes and link read alignment to the reference (Fig. 2A-B). Figure 2C displays the breakpoints of 2p21(36,702,101) and 15q26.1(100,682,799), as well as the chromosome structural rearrangements of t(2;15)(p21;q26.1), all further confirmed through Gap-PCR, gel electrophoresis, and Sanger sequencing (Fig. 3D-E). Both breakpoints were found within the introns of *CRIM1* and *ADAMTS17*, thus disrupting gene structure (Table 1). The rearranged chromosome diagrams of other nine carriers are shown in Supplementary Figs. 1–9, and the involved disrupted genes are presented in Table 1. These results indicate the potential of ViLR for exact breakpoint identification.

An approximately 2 Mbp region flanking upstream and downstream of each breakpoint was selected for informative SNP collection (Supplementary Tables 3–11). Interestingly, the chr13 breakpoint in the PSJ23002 carrier was within a short-arm satellite, a region not detected by ViLR, as this is one of the linked short-read NGS' inherent limitations; thus, the haplotype of this

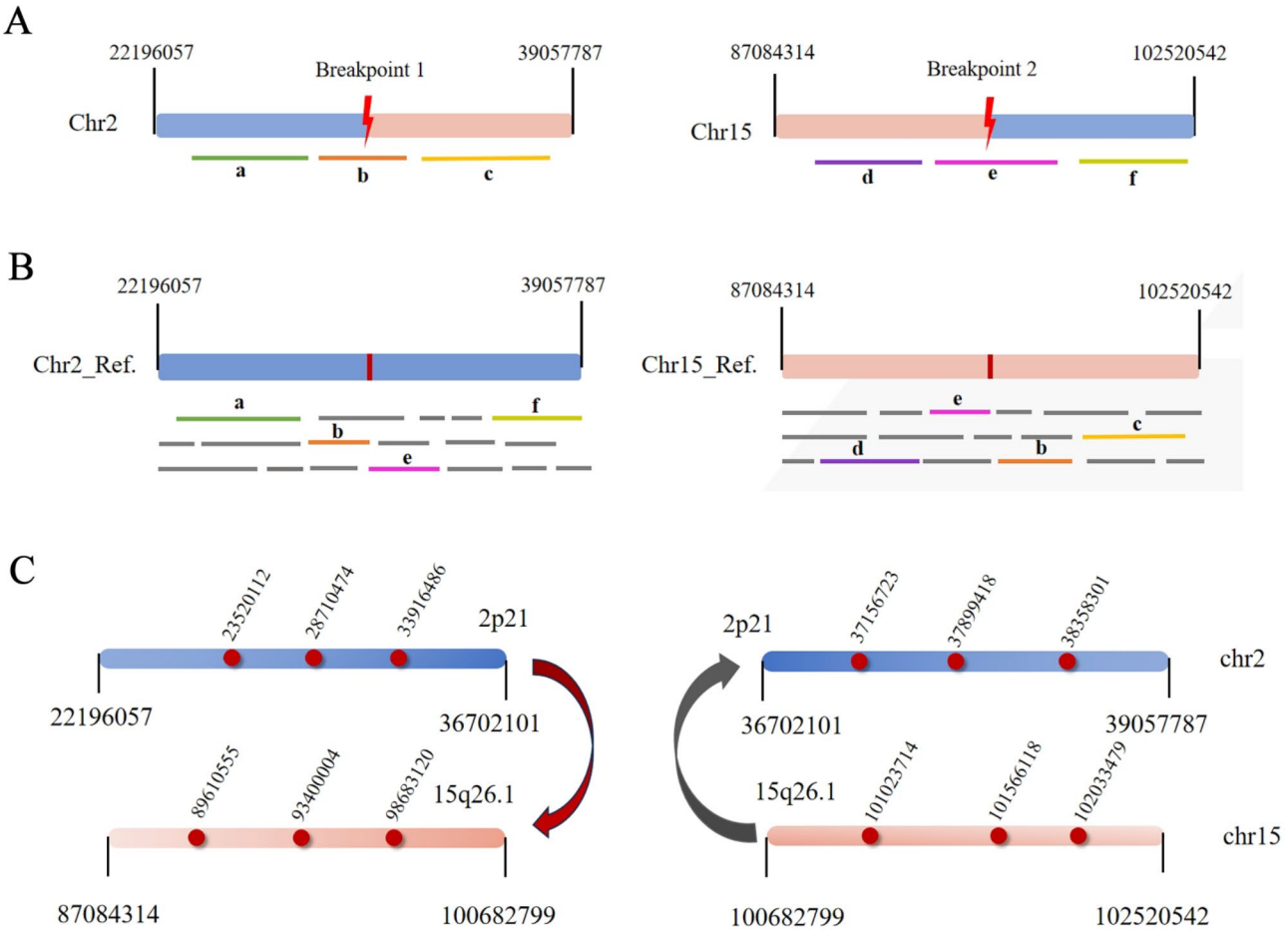

Fig. 2 Diagram of reads config and alignment at the breakpoint regions of PSJ22007 carrier. a–f represent different barcoded beads. (**A**) Each chromosome was inserted with multiple diverse barcoded beads for subsequent sequencing; (**B**) After sequencing, breakpoint locations and chromosome translocations could be precisely detected by ligation of various different barcoded beads and link reads alignment to the reference; (**C**) Breakpoints and rearranged chromosome diagram of the PSJ22007 carrier

breakpoint region was referred to the downstream SNP loci (Supplementary Fig. 3B). The remaining nine carriers all obtained successful haplotype phasing based on both upstream and downstream informative SNP loci per breakpoint (Fig. 3C, Supplementary Figs. 1–9).

Embryo haplotype determination by ViLR

After preclinical carrier's haplotyping, Pedigree PSJ23021 had not yet received ovarian stimulation. Pedigree PSJ22019 and PSJ23002 both underwent two in vitro fertilization cycles, while other seven families only underwent one cycle. A total of 41 blastocysts were subjected to biopsy and WGA. After genome library construction, sequencing and linkage analysis, the haplotype and chromosome structural rearrangements in each embryo could be directly identified based on the established carriers' haplotypes (Fig. 1; Table 2). High-quality control of sequencing data was performed for all embryos (Supplementary Table 2). The average ADO rate of all balanced embryos was only about 6.07%, which indicated that as many informative SNP loci as possible could be obtained on each side of the breakpoint per family for embryo haplotype determination.

Each family with available embryos underwent a single embryo transplantation to date. Out of 40 CNV detected embryos, 18 were euploid, in which 10 were euploid/normal embryos, 7 were euploid/balanced carrier embryos, and the remaining one unknown due to homologous recombination of the breakpoint region (Fig. 3A). Haplotype analysis of pedigree PSJ22007 indicated that E1 was a translocation carrier embryo (Fig. 3B), whose breakpoints were further confirmed through traditional testings (Fig. 3D-E). E2 and E3 both harbored normal haplotypes, thus producing a negative result in breakpoint verification (Fig. 3D). However, E1 was a mosaic embryo and E2 had a trisomy 4; thus, only embryo E3 was suitable for transplantation (Fig. 4A).

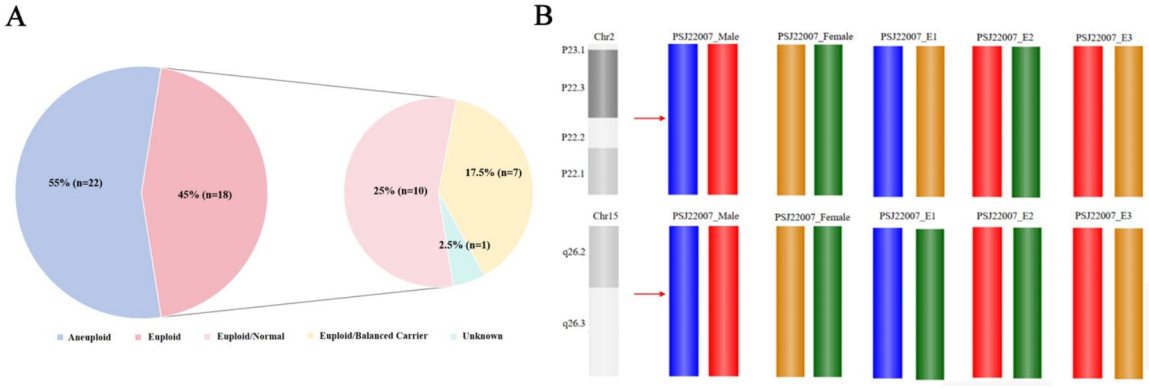

C

Chr2

SNP loci	Male		Female		E1		E2		E3	
	F1	F0	M0	M1	F1	M0/M1	F0	M0/M1	F0	M0/M1
36624914	T	C	C	C	T	C	C	C	C	C
36627725	A	G	G	G	A	G	G	G	G	G
36640405	C	T	T	T	C	T	T	T	T	T
36687670	C	T	T	T	C	T	T	T	T	T
36688921	C	T	A	A	C	A	A	A	A	A
36702100	A	A	A	A	MISS		MISS		MISS	
36702101	T	T	T	T	MISS		MISS		MISS	
36702458	C	A	A	A	C	A	A	A	A	A
36735024	T	G	T	T	T	T	G	T	G	T
36754879	C	T	T	T	C	T	T	T	T	T
36788616	G	A	A	A	G	A	A	A	A	A
36791893	A	G	G	G	A	G	G	G	G	G

Chr15

SNP loci	Male		Female		E1		E2		E3	
	F1	F0	M0	M1	F1	M0/M1	F0	M0/M1	F0	M0/M1
100659756	C	G	C	C	C	C	G	C	G	C
100663329	C	T	C	C	C	C	T	C	T	C
100663362	C	T	C	C	C	C	T	C	T	C
100663405	C	T	C	C	C	C	T	C	T	C
100672715	C	T	C	C	C	C	T	C	T	C
100682799	T	T	T	T	MISS		MISS		MISS	
100682800	A	A	A	A	MISS		MISS		MISS	
100686772	A	G	G	G	A	G	G	G	G	G
100726800	G	C	G	G	G	G	C	G	C	G
100727970	G	C	G	G	G	G	C	G	C	G
100728149	C	T	C	C	C	C	T	C	T	C
100735352	G	A	G	G	G	G	A	G	A	G

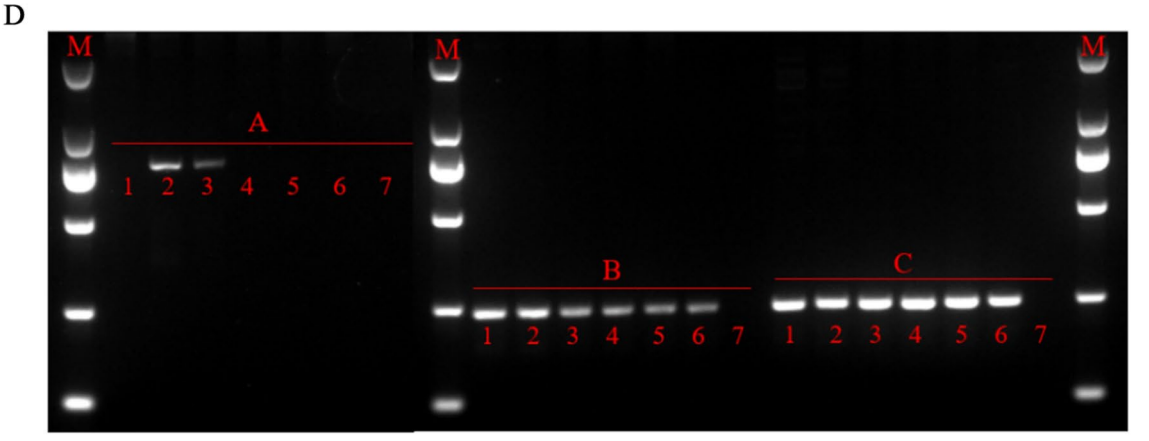

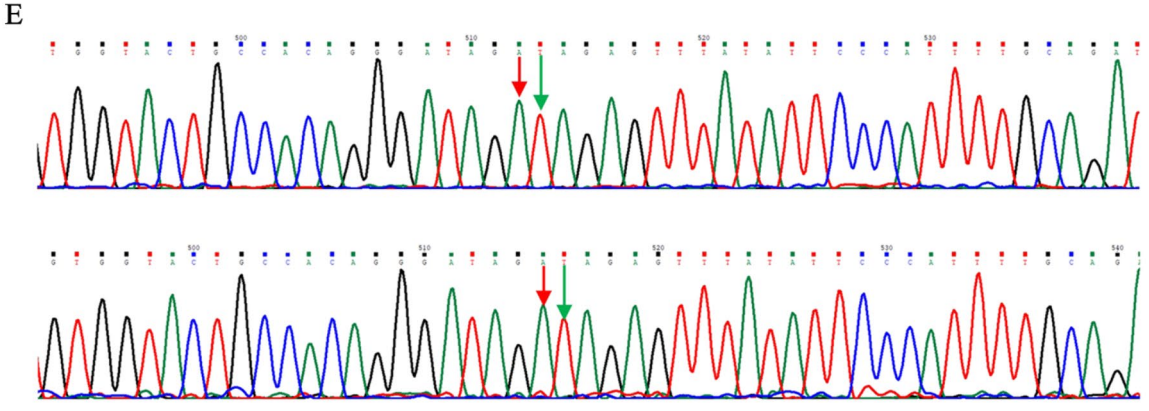

Fig. 3 (See legend on next page.)

(See figure on previous page.)

Fig. 3 SNP haplotype and breakpoint confirmation of pedigree PSJ22007. (**A**) Out of 40 CNV detected embryos, 22 were aneuploid (dark blue), 18 were euploid (dark pink), in which 10 were euploid/normal embryos (light pink), 7 were euploid/balanced carrier embryos (light yellow), and the remaining one unknown (light blue); (**B**) **Haplotype diagram flanking breakpoint regions of t(2;15)(p21;q26.1) in pedigree PSJ22007.** The gray single chain is the normal chain from female in this family. Red represent the carrier's normal single chain and blue the paternal carrying chain. Yellow and green indicate the maternal normal single chains. PSJ22007_E1 exhibited the carrier chain color in the effective diploid region near the breakpoints of chr2 and chr15, that was translocation carrier embryo. Both PSJ22007_E2 and PSJ22007_E3 showed normal chain color in the effective diploid region near those breakpoints, being thus normal embryos. The red arrow indicates the targeted position; (**C**) Examples of informative SNP loci flanking upstream and downstream of two breakpoints in pedigree PSJ22007. The red bold font and pentagram indicate the fracture point region. F0 represent the male's normal chromatid in red, F1 the male's translocation chromatid in blue, both M0 and M1 the maternal normal chromatids in yellow and green; (**D**) Gel analysis of Gap-PCR products. A–C different groups with different primer pairs. The primer sequences and corresponding chromosomal locations are shown in Supplemental Table 12. M: DL2000 Marker; No. 1: PSJ22007 normal female; No. 2: PSJ22007 male carrier; No. 3: PSJ22007_E1; No. 4: PSJ22007_E2; No. 5: PSJ22007_E3; No. 6: the negative control; No. 7: no template control; (E) Sanger sequencing of PSJ22007 male carrier and PSJ22007_E1. The red arrow indicates the breakpoint of 2p21(36,702,101), and the green arrow that of 15q26.1(100,682,799)

Clinical outcomes of PGT-SR

Thanks to successful preclinical ViLR application, one optimal embryo was finally selected and transplanted in each of the seven families (Table 2). Four pedigrees of PSJ22007, PSJ23008, PSJ23011 and PSJ23012 had finished amniocentesis, and obtained normal cytogenetic results, concordant with ViLR analysis data (Fig. 4B and D, Supplementary Figs. 1–9). Unfortunately, Pedigree PSJ23019 lost their baby at seven weeks of gestational age. To exclude lethal monogenic disorders or chromosome anomalies, enhanced whole exome sequencing combined with copy number variation (CNV) detection was performed in abortive villi, but no genetic causes were identified. At the time of writing this manuscript, four women had received prenatal diagnosis, each of them eventually delivered a healthy baby with normal phenotypes.

Discussion

PGT-SR has been widely regarded as a valuable technology to provide diagnosis and genetic counsel for CSR couples [20, 21]. CSR families could generally have a good clinical outcome after euploid/normal or euploid/balanced embryo transfer, however, multiple complex factors affecting chromosome segregation during the process of mitosis and meiosis, would limit the number of embryos available for transfer. A retrospective study by Ogur et al. in 300 PGT-SR couples discovered that the most important factors that affect segregations and the proportion of transferable embryos were chromosomal rearrangement type and sex [22]. Another study comparing three different PGT-SRs using the NGS method demonstrated that the percentage of unbalanced blastocysts was significantly higher in reciprocal translocation than in inversion and Robertsonian translocation carriers (64.31% vs. 28.05% vs. 37.02%) [23]. Besides, DNA elimination, centromeric and centromere-proximal features, chromosome size and location, etc., all could increase non-random chromosome segregation errors [24, 25], further exacerbating fertility risks. In other words, unblanced chromosomal rearrangement-induced abnormal embryonic development, abortion, stillbirth, and even severe birth defects will be unavoidable if no any interventions are adopted for carriers.

The application of haplotyping for embryonic PGT-SR, rather than direct embryo detection, makes a valuable technological contribution to ART. In traditional PGT phase, short read dependent haplotype construction requires simultaneous detection of samples from other family members or diseased offspring other than husband and wife, in order to evaluate whether embryos inherit parental pathogenic chains. In fact, many families do not have a proband sample or complete family members, so haplotype analysis without a proband is needed. Here in our study, ViLR provides an effective solution for these specific couples, which analysis is based on NGS platform, and does not require a proband. Its virtual long read capacity can be effectively applied for breakpoint identification and direct SNP haplotyping in *de novo* PGT-SR carriers.

Although two different NGS-based linked-read solutions, respectively named HLRS [26] and Phbol-seq [27], have been recently reported for proband-independent carrier's haplotyping in preclinical PGT-M, only two or three families were separately included, and their use for clinical PGT-SR is insufficient. In this study, we accurately detected the breakpoints in 10 *de novo* CSR carriers using ViLR, which facilitated subsequent clinical PGT-SR and genetic counseling. Nine families obtained embryos via ICSI, which were sequenced and phased to determine their suitability for implantation. Among those, five euploid/normal embryos and two euploid/balanced carrier embryos were selected for transplantation. Four pedigrees already gave birth to healthy babies, and one woman from pedigree PSJ24002 continued to have uneventful pregnancy till now.

Compared to traditional testing approaches, such as fluorescence in situ hybridization (FISH), array comparative genomic hybridization, SNP arrays, karyomapping, etc., the linked short-read NGS has higher-resolution, higher-accuracy, low-cost [28, 29], and is regarded as a widely acceptable method for PGT-SR. Despite several successful applications of LRS in clinical PGT-SR owing to its unique capacity of long reads [13–15, 30], both

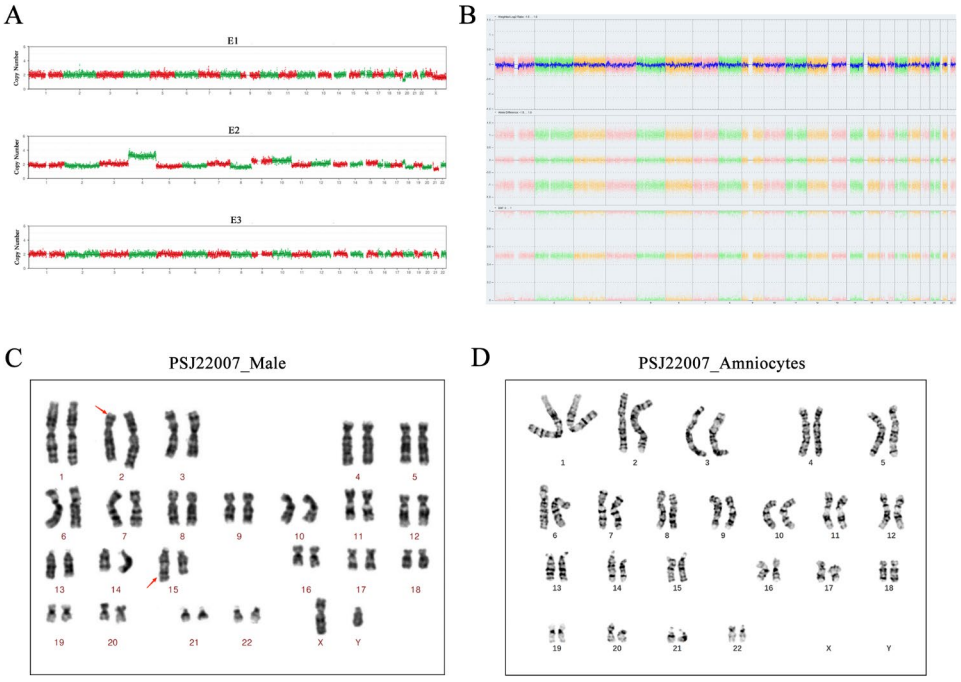

Fig. 4 Embryonic CNV results and prenatal cytogenetic results of pedigree PSJ22007. (**A**) CNV results of embryos. PSJ22007_E1 was a mosaic embryo involving chr20 and chrX, PSJ22007_E2 had Trisomy 4, and only PSJ22007_E3 was an euploid embryo. Detailed CNVs results are shown in Table 2; (**B**) CMA result of prenatal amniocytes; (**C**) KT result of the PSJ22007 male carrier. The red arrow indicates the translocation chromatid of chr2 and chr15; (**D**) KT result of PSJ22007 prenatal amniocytes

PacBio and ONT still had their inherent limitations. According to Wenger's study, the optimization of circular consensus sequencing method could improve the accuracy of PacBio and generate highly accurate (99.8%) long HiFi reads [31], which indicated Pacbio's relatively low error rate. However, Pacbio was still not recommended for long fragment assembly and carrier haplotype construction in practical scenario, because its average fragment length is only about 10-20Kb (e.g. an average length of 13.5 kb in Wenger's study), and the assembled N50 value of ~150Kb is lower than ONT (~800Kb) and ViLR (11-16 Mb). In addition, the ONT fragment length displayed a large variation, and its error rate was reported up to 5–15% [32–34], thus the low base mass could lead to less informative SNPs, that was insufficient for haplotype phasing. So the argument for increased diagnostic yield of LRS remains further validated, and it is not reliable to replace the previous NGS sequencing devices.

To our knowledge, FISH could only detect specific chromosomal regions or probes, thus resulting in limited coverage, which could not comprehensively reveal the whole chromosomal SVs. Therefore, preimplantation genetic testing for aneuploidy (PGT-A) cannot be simultaneously detected by FISH in PGT-SR scenario [35], thus aneuploidies and mosaicisms cannot be fully excluded, which limitation could be solved by NGS technology instead. Also, the interpretation of FISH results relies on the experience and ability of the operator, whose subjectivity may lead to data inaccuracies. Furthermore, although the cost of FISH technology is relatively low, the overall cost will also increase significantly as more chromosomal regions are required to be detected. In contrast, NGS-based haplotype construction technology offers higher resolution and accuracy, and can comprehensively uncover all chromosomal SVs, including small deletions/duplications, inversions, or translocations, etc., providing more detailed information for genetic counseling and fertility planning. Additionally, NGS technology features high throughput, allowing for the processing of a large number of samples in a short period, enhancing detection efficiency. Although the initial investment and operating costs of NGS technology is higher, its long-term benefits and accuracy got priority consideration in many genetic counseling and reproductive health fields.

Here, NGS-based ViLR technology provides a more comprehensive and accurate solution for PGT-SR. The mean Q30 rate of ViLR analysis is over 90%, which is comparable to the mean base quality of other NGS platform [36], thus lower error was generated. A MGI-2000 sequencer (MGI Tech Co., Ltd., ShenZhen, China) was used in this study for ViLR sequencing, which indicated an extremely lower sequencing cost per gigabase (Gb) of data compared to LRS platforms (ViLR: $6/Gb, vs. Pacbio: $30/Gb, vs. Nanopore: $24/Gb) from our local investigation. In addition to the direct sequencing costs, other regional cost differences should also be considered,

which influence factors mainly included regional economic levels, price index, and the prevalence of sequencing technology. For example, in highly developed regions, although sequencing technology may be more advanced, the corresponding equipment and labor costs are also higher; Instead, in some emerging or developing countries, the cost may be relatively low as sequencing technology becomes more widely available. Economies of scale also have an impact on sequencing costs. Large-scale sequencing projects tend to be more cost-effective because fixed costs (e.g., equipment acquisition, laboratory construction) can be spread over more samples, thus reducing the cost per sequencing unit. This scale plays an important role in driving the adoption of sequencing technology and reducing health care costs. Of course, indirect costs, including data interpretation, cannot be ignored. These costs, although not directly reflected in the sequencing process, are equally important to patients and health care organizations. Therefore, all relevant factors are needed to be considered comprehensively to ensure the accuracy and feasibility of medical decisions when conducting cost analysis. Furthermore, due to the more extensive clinical application of NGS, the cost-effectiveness and adoption of ViLR technology can be potentially enhanced in the future. Using the same barcoded labeling, ViLR enables sequencing longer DNA fragments with an average length of over 30 Kb, and generates an assembled N50 block size of up to 16 Mb, which indicates that ViLR can span larger chromosomal regions, detect more complex SVs across the whole genome, including complex translocations, cryptic translocations, large inversions and deletions. We did not enroll any complex rearranged cases in this prospective study, that testing performance using ViLR would be summarized in our future study.

Similar to LRS, ViLR analysis was able to generate direct informative SNP profiles phased against the breakpoints. In this study, 98% of the whole genome regions could be covered and > 3.8 million SNPs were obtained for carriers, facilitating more accurate haplotype construction. Similarly, for embryos, 99.8% of targeted regions were mapped and 1 million SNPs were detected, data sufficient for genome-wide linkage analysis. Also, MDA was used for WGA of embryo biopsies in our study, by which a lower ADO rate (average 6.07%) and more informative SNP loci [9, 28, 37] were achieved for embryo haplotype determination.

In our study, a total of 18 euploid embryos were obtained, of which 10 were euploid/normal embryos, 7 were euploid/balanced carrier embryos, and the remaining unknown phasing was due to homologous recombination of the breakpoint region. Homologous recombination is an important process in biology that involves the exchange and recombination of DNA. In PGT phase, homologous recombination may have a certain impact on the test results. Since a constant background recombination rate of 1 cM/Mb in human genome [38], the homologous recombination near the chromosomal breakpoint cannot be excluded, which may result in inaccurate detection results in the embryos. However, analysis of sufficient effective SNP sites facilitates the identification of embryonic recombination. ViLR provides an average of more than 5 SNP loci flanking upstream and downstream of each breakpoint within an approximately 1 Mbp region, that accurate haplotyping event can effectively distinguish the recombination region. Certainly, more clinical practical verification is needed to clarify the effectiveness of ViLR technology for detection of embryonic homologous recombination, which will also provide more useful information for doctors to select better embryos for transfer.

Nevertheless, ViLR still had conventional linked short-read NGS's limitations for PGT-SR [39, 40]. It cannot detect Robertsonian translocation and high-repeat areas [41]. SVs near the telomer, in the centromere and satellite regions, or in GC-rich regions, cannot be detected by linked short-read NGS [42, 43], but could be reasonably and effectively tested by optical genome mapping [44, 45] or third-generation LRS [46, 47]. Accordingly, the SNP haplotype of the chr13 breakpoint region in the PSJ23002 carrier could not be directly detected by ViLR owing to its satellite area. Similar to LRS, a higher requirement of sample DNA quality (90% of DNA ≥ 10 kb & 50% of DNA > 30 kb) is needed for ViLR, because the length of inserted-barcode DNAs determine the detectability and precision of this method. Certainly, this requires sample conservation and transport at -20°C and to avoid repeated freeze-thaw. Additionally, in ViLR analysis, heterozygous SNPs in the carrier and homozygous SNPs in the other partner were selected for informative SNP collection. Haplotype phasing could be limited when the breakpoint is within an extended region of homozygosity, which is also compromised by LRS detection [13]. Thus, unbalanced reference embryo could be used for haplotype linkage analysis in this particular case. Therefore, the combination of ViLR and traditional testing is necessary for targeting those specific genome sequences.

All carriers in this study were confirmed as balanced translocation or inversion carriers using peripheral karyotyping. Actually, germline mosaicism can not be entirely excluded in our cohort. The possibility of mosaicism exists, although its probability is relatively low (~ 5%) [48, 49]. Germline mosaicism may be caused by multiple factors, such as gene mutation during the development of the fertilized oocyte, chromosome non-separation, germ cell fusion, etc. In addition, environmental factors (e.g. radiation, chemicals, etc.) may also affect the genetic stability of germ cells, thereby increasing the risk

of germline mosaicism. However, due to the complexity and diversity of germline mosaicism, the research on its mechanism, detection methods and clinical significance is still not enough. It is difficult to construct the carrying haplotype of parents when more pathogenic variants occured in germ cells, but less existed in peripheral blood. Increasing the depth of long fragment sequencing may achieve successful haplotype. Therefore, we need to keep an open and cautious attitude towards the inaccuracy of test results caused by germline mosaicism during PGT detection, which also warrants further exploration.

Overall, our prospective study using a novel ViLR platform identified precise breakpoints and achieved embryonic diagnosis for 10 *de novo* CSR couples. We obtained full agreement between prenatal cytogenetic results and ViLR data in four pedigrees. Further, direct SNP haplotyping via ViLR did not require proband or other familial analysis. Four healthy babies' born thus far further validates the potential of ViLR as a feasible tool for future clinical *de novo* PGT-SR. Of course, postnatal clinical examinations are needed to ensure the agreement between genetic diagnosis and clinical outcomes. However, given the small sample size of our study, the accuracy and testing scope of this technology require further testing in larger sample sizes and multiple centers.

Conclusions

Here, we developed ViLR, a novel virtual NGS-based long read method, and demonstrated its clinical relevance for breakpoint identification and direct SNP haplotyping in 10 *de novo* CSR carriers. Our data provide a novel solution in *de novo* PGT-SR families without proband or other inheritance information available.

Abbreviations

LRS	Long Read Sequencing
PGT-SR	Preimplantation Genetic Testing for Structural Rearrangement
ViLR	Virtual NGS-based Long Read Method
CSR	Chromosomal Structural Rearrangements
BT	Balanced Translocation
ART	Assisted Reproductive Technology
NGS	Next-Generation Sequencing
SNP	Single Nucleotide Polymorphism
WGS	Whole Genome Sequencing
ADO	Allelic Dropout
WGA	Whole Genome Amplification
PacBio	Pacific Biosciences
ONT	Oxford Nanopore Technologies
PGT-M	Preimplantation Genetic Testing for Monogenic Disease
ICSI	Intracytoplasmic Sperm Injection
KT	Karyotyping
HMW	High Molecular Weight
SV	Structural Variant
MDA	Multiple Displacement Amplification
CNV	Copy Number Variation
FISH	Fluorescence In Situ Hybridization
PGT-A	Preimplantation Genetic Testing for Aneuploidy

Supplementary Information

The online version contains supplementary material available at https://doi.org/10.1186/s12958-025-01366-3.

Supplementary Material 1
Supplementary Material 2
Supplementary Material 3
Supplementary Material 4
Supplementary Material 5
Supplementary Material 6
Supplementary Material 7
Supplementary Material 8
Supplementary Material 9
Supplementary Material 10
Supplementary Material 11
Supplementary Material 12
Supplementary Material 13
Supplementary Material 14
Supplementary Material 15

Acknowledgements

We thank all participants in this study.

Author contributions

All authors fulfill the criteria for authorship. JYX, CSC and HBL conceptualized and designed the manuscript; JYX and MX drafted initial manuscript; JYX, MX, JC, KK, MNG, ML, HYS, XZ, LYC and BL participated in data acquisition, analysis and interpretation; LMZ, CSC, and HBL were involved in project administration. MX, CSC and HBL provided the funding supporting; CSC and HBL contributed to the article revision. All authors approved the final version of the manuscript and agreed accountable for all aspects of this work.

Funding

This work was supported by grants from Ningbo science and technology project (No.2023Z178), the Social Development Public Welfare Foundation of Ningbo (No.2022S035), Innovation Project of Distinguished Medical Team in Ningbo (No.2022020405), Medical and Health Project of Zhejiang province (No.2022KY1157), Key Technology Breakthrough Program of 'Ningbo Sci-Tech Innovation YONGJIANG 2035' (No.2024Z221), Ningbo Medical and HealthBrand Discipline (PPXK2024-06).

Data availability

No datasets were generated or analysed during the current study.

Declarations

Ethics approval and consent to participate

Written informed consent was obtained from all participants, and this study was approved by the IRB of the Affiliated Women and Children's Hospital of Ningbo University (No. EC2020-048).

Consent for publication

All of the authors have consented to publication of this research. All patients have consented to publication of this research.

Competing interests

The authors declare no competing interests.

Author details
[1]The Central Laboratory of Birth Defects Prevention and Control, The Affiliated Women and Children's Hospital of Ningbo University, Ningbo, Zhejiang 315012, China
[2]Ningbo Key Laboratory for the Prevention and Treatment of Embryogenic Diseases, The Affiliated Women and Children's Hospital of Ningbo University, 339 Liuting Street, Haishu District, Ningbo, Zhejiang 315012, China
[3]Ningbo Key Laboratory of Genomic Medicine and Birth Defects Prevention, The Affiliated Women and Children's Hospital of Ningbo University, Ningbo, Zhejiang 315012, China
[4]Center for Reproductive Medicine, The Affiliated Women and Children's Hospital of Ningbo University, Ningbo, Zhejiang 315012, China
[5]Basecare Medical Device Co., Ltd, Suzhou, Jiangsu 215028, China
[6]State Key Laboratory of Microbial Metabolism, Joint International Research Laboratory of Metabolic and Developmental Sciences, School of Life Sciences and Biotechnology, Shanghai Jiao Tong University, Shanghai 200240, China

Received: 12 December 2024 / Accepted: 14 February 2025
Published online: 05 March 2025

References

1. Clementini E, Palka C, Iezzi I, Stuppia L, Guanciali-Franchi P, Tiboni GM. Prevalence of chromosomal abnormalities in 2078 infertile couples referred for assisted reproductive techniques. Hum Reprod. 2005;20:437–42.
2. Anton E, Vidal F, Egozcue J, Blanco J. Genetic reproductive risk in inversion carriers. Fertil Steril. 2006;85:661–6.
3. Yuan J, Jin L, Wang M, Wei S, Zhu G, Xu B. Detection of chromosome aberrations in 17054 individuals with fertility problems and their subsequent assisted reproductive technology treatments in central China. Hum Reprod. 2023;38:ii34–46.
4. Wilch ES, Morton CC. Historical and clinical perspectives on chromosomal translocations. Adv Exp Med Biol. 2018;1044:1–14.
5. Morin SJ, Eccles J, Iturriaga A, Zimmerman RS. Translocations, inversions and other chromosome rearrangements. Fertil Steril. 2017;107:19–26.
6. Viotti M. Preimplantation genetic testing for chromosomal abnormalities: aneuploidy, mosaicism, and structural rearrangements. Genes (Basel) 2020; 11.
7. Chow J, Yeung W, Lee V, Lau E, Ng E. Evaluation of preimplantation genetic testing for chromosomal structural rearrangement by a commonly used next generation sequencing workflow. Eur J Obstet Gynecol Reprod Biol. 2018;224:66–73.
8. Treff NR, Northrop LE, Kasabwala K, Su J, Levy B, Scott RJ. Single nucleotide polymorphism microarray-based concurrent screening of 24-chromosome aneuploidy and unbalanced translocations in preimplantation human embryos. Fertil Steril. 2011;95:1606–12.
9. De Witte L, Raman L, Baetens M, De Koker A, Callewaert N, Symoens S, Tilleman K, Vanden MF, Dheedene A, Menten B. Gentype: all-in-one preimplantation genetic testing by pedigree haplotyping and copy number profiling suitable for third-party reproduction. Hum Reprod. 2022;37:1678–91.
10. Yuan P, Xia J, Ou S, Liu P, Du T, Zheng L, Yin X, Xie L, Zhang S, Yan H, Gao Y, Zhang Q, Jiang H, Chen F, Wang W. A whole-genome sequencing-based novel preimplantation genetic testing method for de novo mutations combined with chromosomal balanced translocations. J Assist Reprod Genet. 2020;37:2525–33.
11. Chen S, Yin X, Zhang S, Xia J, Liu P, Xie P, Yan H, Liang X, Zhang J, Chen Y, Fei H, Zhang L, Hu Y, Jiang H, Lin G, Chen F, Xu C. Comprehensive preimplantation genetic testing by massively parallel sequencing. Hum Reprod. 2021;36:236–47.
12. Ou Z, Deng Y, Liang Y, Chen Z, Sun L. Using affected embryos to establish linkage phase in preimplantation genetic testing for thalassemia. Reprod Biol Endocrinol. 2022;20:75.
13. Yu MMY, Ma Q, Wang M, Tian H, Zhang S, Liu WMMJ, Yang Y, Pan Q, Liang X, Wang H, Leigh L, Cram D DS and, Yao Y. Variant haplophasing by long-read sequencing: a new approach to preimplantation genetic testing workups. Fertil Steril. 2021;116:774–83.
14. Zhang S, Liang F, Lei C, Wu J, Fu J, Yang Q, Luo X, Yu G, Wang D, Zhang Y, Lu D, Sun X, Liang Y, Xu C. Long-read sequencing and haplotype linkage analysis enabled preimplantation genetic testing for patients carrying pathogenic inversions. J Med Genet. 2019;56:741–9.
15. Pei Z, Deng K, Lei C, Du D, Yu G, Sun X, Xu C, Zhang S. Identifying balanced chromosomal translocations in human embryos by oxford nanopore sequencing and breakpoints region analysis. Front Genet. 2021;12:810900.
16. Tsuiko O, El AY, Jatsenko T, Allemeersch J, Melotte C, Ding J, Debrock S, Peeraer K, Vanhie A, De Leener A, Pirard C, Kluyskens C, Denayer E, Legius E, Vermeesch JR, Brems H, Dimitriadou E. Preclinical workup using long-read amplicon sequencing provides families with de novo pathogenic variants access to universal preimplantation genetic testing. Hum Reprod. 2023;38:511–9.
17. Xiao T, Zhou W. The third generation sequencing: the advanced approach to genetic diseases. Transl Pediatr. 2020;9:163–73.
18. Iscn. 2024 - an international system for human cytogenomic nomenclature (2024). Cytogenet Genome Res 2024; 164: 1-224.
19. Xie P, Hu X, Kong L, Mao Y, Cheng D, Kang K, Dai J, Zhao D, Zhang Y, Lu N, Wan Z, Du R, Xiong B, Zhang J, Tan Y, Lu G, Gong F, Lin G, Liang B, Du J, Hu L. A novel multifunctional haplotyping-based preimplantation genetic testing for different genetic conditions. Hum Reprod. 2022;37:2546–59.
20. Takeuchi K. Pre-implantation genetic testing: past, present, future. Reprod Med Biol. 2021;20:27–40.
21. Fesahat F, Montazeri F, Hoseini SM. Preimplantation genetic testing in assisted reproduction technology. J Gynecol Obstet Hum Reprod. 2020;49:101723.
22. Ogur C, Kahraman S, Griffin DK, Cinar YC, Tufekci MA, Cetinkaya M, Temel SG, Yilmaz A. Pgt for structural chromosomal rearrangements in 300 couples reveals specific risk factors but an interchromosomal effect is unlikely. Reprod Biomed Online. 2023;46:713–27.
23. Yuan P, Zheng L, Ou S, Zhao H, Li R, Luo H, Tan X, Zhang Q, Wang W. Evaluation of chromosomal abnormalities from preimplantation genetic testing to the reproductive outcomes: a comparison between three different structural rearrangements based on next-generation sequencing. J Assist Reprod Genet. 2021;38:709–18.
24. Budrewicz J, Chavez SL. Insights into embryonic chromosomal instability: mechanisms of dna elimination during mammalian preimplantation development. Front Cell Dev Biol. 2024;12:1344092.
25. Klaasen SJ, Kops G. Chromosome inequality: causes and consequences of non-random segregation errors in mitosis and meiosis. Cells 2022; 11.
26. Li Q, Mao Y, Li S, Du H, He W, He J, Kong L, Zhang J, Liang B, Liu J. Haplotyping by linked-read sequencing (hlrs) of the genetic disease carriers for preimplantation genetic testing without a proband or relatives. Bmc Med Genomics. 2020;13:117.
27. Zhang P, Zhao X, Li Q, Xu Y, Cheng Z, Yang L, Wang H, Tao Y, Huang G, Wu R, Zhou H, Zhao S. Proband-independent haplotyping based on ngs-based long-read sequencing for detecting pathogenic variant carrier status in preimplantation genetic testing for monogenic diseases. Front Mol Biosci. 2024;11:1329580.
28. Yin X, Tan K, Vajta G, Jiang H, Tan Y, Zhang C, Chen F, Chen S, Zhang C, Pan X, Gong C, Li X, Lin C, Gao Y, Liang Y, Yi X, Mu F, Zhao L, Peng H, Xiong B, Zhang S, Cheng D, Lu G, Zhang X, Lin G, Wang W. Massively parallel sequencing for chromosomal abnormality testing in trophectoderm cells of human blastocysts. Biol Reprod. 2013;88:69.
29. Zhang S, Zhao D, Zhang J, Mao Y, Kong L, Zhang Y, Liang B, Sun X, Xu C. Basephasing: a highly efficient approach for preimplantation genetic haplotyping in clinical application of balanced translocation carriers. Bmc Med Genomics. 2019;12:52.
30. Liu S, Wang H, Leigh D, Cram DS, Wang L, Yao Y. Third-generation sequencing: any future opportunities for pgt? J Assist Reprod Genet. 2021;38:357–64.
31. Wenger AM, Peluso P, Rowell WJ, Chang PC, Hall RJ, Concepcion GT, Ebler J, Fungtammasan A, Kolesnikov A, Olson ND, Topfer A, Alonge M, Mahmoud M, Qian Y, Chin CS, Phillippy AM, Schatz MC, Myers G, Depristo MA, Ruan J, Marschall T, Sedlazeck FJ, Zook JM, Li H, Koren S, Carroll A, Rank DR, Hunkapiller MW. Accurate circular consensus long-read sequencing improves variant detection and assembly of a human genome. Nat Biotechnol. 2019;37:1155–62.
32. Rang FJ, Kloosterman WP, de Ridder J. From squiggle to basepair: computational approaches for improving nanopore sequencing read accuracy. Genome Biol. 2018;19:90.
33. Kono N, Arakawa K. Nanopore sequencing: review of potential applications in functional genomics. Dev Growth Differ. 2019;61:316–26.
34. Lin B, Hui J, Mao H. Nanopore technology and its applications in gene sequencing. Biosens (Basel) 2021; 11.

35. Carvalho F, Coonen E, Goossens V, Kokkali G, Rubio C, Meijer-Hoogeveen M, Moutou C, Vermeulen N, De Rycke M. Eshre pgt consortium good practice recommendations for the organisation of pgt. Hum Reprod Open. 2020; 2020: hoaa21.
36. Sun Y, Zhao X, Fan X, Wang M, Li C, Liu Y, Wu P, Yan Q, Sun L. Assessing the impact of sequencing platforms and analytical pipelines on whole-exome sequencing. Front Genet. 2024;15:1334075.
37. He F, Zhou W, Cai R, Yan T, Xu X. Systematic assessment of the performance of whole-genome amplification for snp/cnv detection and beta-thalassemia genotyping. J Hum Genet. 2018;63:407–16.
38. Hassan S, Surakka I, Taskinen MR, Salomaa V, Palotie A, Wessman M, Tukiainen T, Pirinen M, Palta P, Ripatti S. High-resolution population-specific recombination rates and their effect on phasing and genotype imputation. Eur J Hum Genet. 2021;29:615–24.
39. Alkan C, Sajjadian S, Eichler EE. Limitations of next-generation genome sequence assembly. Nat Methods. 2011;8:61–5.
40. Abbasi A, Alexandrov LB. Significance and limitations of the use of next-generation sequencing technologies for detecting mutational signatures. Dna Repair (Amst). 2021;107:103200.
41. Giuliano R, Maione A, Vallefuoco A, Sorrentino U, Zuccarello D. Preimplantation genetic testing for genetic diseases: limits and review of current literature. Genes (Basel) 2023; 14.
42. Goodwin S, Mcpherson JD, Mccombie WR. Coming of age: ten years of next-generation sequencing technologies. Nat Rev Genet. 2016;17:333–51.
43. Korbel JO, Urban AE, Affourtit JP, Godwin B, Grubert F, Simons JF, Kim PM, Palejev D, Carriero NJ, Du L, Taillon BE, Chen Z, Tanzer A, Saunders AC, Chi J, Yang F, Carter NP, Hurles ME, Weissman SM, Harkins TT, Gerstein MB, Egholm M, Snyder M. Paired-end mapping reveals extensive structural variation in the human genome. Science. 2007;318:420–6.
44. Garcia-Heras J. Optical genome mapping: a revolutionary tool for next generation cytogenomics analysis with a broad range of diagnostic applications in human diseases. J Assoc Genet Technol. 2021;47:191–200.
45. Shi S, Huang P, Yan R, Li R. Identification of complex and cryptic chromosomal rearrangements by optical genome mapping. Mol Cytogenet. 2023;16:5.
46. Wu Z, Jiang Z, Li T, Xie C, Zhao L, Yang J, Ouyang S, Liu Y, Li T, Xie Z. Structural variants in the Chinese population and their impact on phenotypes, diseases and population adaptation. Nat Commun. 2021;12:6501.
47. Zhou A, Lin T, Xing J. Evaluating nanopore sequencing data processing pipelines for structural variation identification. Genome Biol. 2019;20:237.
48. Fan L, Wu J, Wu Y, Shi X, Xin X, Li S, Zeng W, Deng D, Feng L, Chen S, Xiao J. Analysis of chromosomal copy number in first-trimester pregnancy loss using next-generation sequencing. Front Genet. 2020;11:545856.
49. Lund I, Becher N, Christensen R, Petersen OB, Steffensen EH, Vestergaard EM, Vogel I. Prevalence of mosaicism in uncultured chorionic villus samples after chromosomal microarray and clinical outcome in pregnancies affected by confined placental mosaicism. Prenat Diagn. 2020;40:244–59.

Publisher's note